ISSN 0915-633X

NATIONAL INSTITUTE FOR FUSION SCIENCE

Implicit CIP (Cubic-Interpolated Propagation) Method in One Dimension

M. Ida and T. Yabe

(Received - May 15, 1995)

NIFS-358 May 1995

RESEARCH REPORT
NIFS Series

NAGOYA, JAPAN

Implicit CIP (Cubic-Interpolated Propagation) Method in One Dimension

Masato IDA and Takashi YABE

Department of Energy Sciences, The Graduate school at Nagatsuta, Tokyo Institute of Technology

4259 Nagatsuta, Midori-Ku, Yokohama 227, Japan

Abstract

A new implicit numerical solver for hyperbolic equations is proposed. This method is based on the CIP (Cubic-Interpolated Propagation) method that was proposed in an explicit form. Both a physical quantity and its spatial derivative are determined so as to obey the given equation. Just same as the CIP method, this method provides a stable and less diffusive result although it has an implicit form. Most importantly, this method, like other implicit schemes, is stable even in a high-CFL computation. In addition, this scheme can be directly solved by non-iterative procedure because of the two-points connected systems although it has third-order accuracy. The scheme is applied to a one-dimensional shock-tube problem accompanied by a region expanding with quite a high velocity.

Keywords Numerical solver, Hyperbolic equation, CIP method, Implicit scheme, Two-points connected systems

1. Introduction

The CIP (Cubic-Interpolated Propagation) method was proposed by one of the authors in 1985 [1] and has been highly proven to be a universal hyperbolic solver in the past decade [2 – 4]. In this method, the spatial profile within each grid is interpolated with a cubic polynomial, and both the value and its spatial derivatives are predicted in advance. This method provides a stable and less diffusive result without any artificial flux treatment commonly used in modern schemes, and can be easily applied to various problems which include linear, nonlinear, and coupled hyperbolic-parabolic equations. However, according as applications have become more general, the fact that the CIP method is limited to a framework of explicit schemes has become an important issue that must be overcome. For a certain application, the use of an explicit scheme is extremely inefficient. For example, a part of the fluid moves very quickly but we do not need accurately solve this part. Even in this case, the calculation time step is controlled by this region when only an explicit solver is available. In order to solve this problem, various kinds of implicit schemes have been proposed [5 – 8]. In this letter, we propose an implicit version of the CIP method.

2. Brief review of the CIP method

Before we come to the main question, we first review the one-dimensional CIP method. Let us consider a linear hyperbolic equation;

$$\frac{\partial f}{\partial t} + c\frac{\partial f}{\partial x} = 0. \tag{1}$$

The solution of this equation is $f(x, t) = f(x - ct, 0)$ if c is constant. Even in the cases where c is not constant and/or there are other non-advective terms, the solution can be estimated as

$$f(x,t+\Delta t) \cong f(x-c\Delta t,t), \qquad (2)$$

during a very short period Δt. In the CIP method, a cubic interpolation is used to estimate $f(x - c\Delta t,\ t)$ when $x - c\Delta t$ is not located at grid points. Thus $f(x)$ is interpolated between x_{i-1} and x_i with a cubic polynomial:

$$F_i(x) = a_i X^3 + b_i X^2 + f_i' X + f_i, \qquad (3)$$

where f_i and f'_i are the values and the first spatial derivatives of f at x_i, and $X = x - x_i$. Two parameters a_i and b_i in eq. (3) are determined from the continuity of f and f' at x_{i-1} as follows:

$$a_i = \frac{(f_i' + f_{i-1}')}{\Delta x^2} - \frac{2(f_i - f_{i-1})}{\Delta x^3}, \qquad (4)$$

$$b_i = \frac{(2f_i' + f_{i-1}')}{\Delta x} - \frac{3(f_i - f_{i-1})}{\Delta x^2}, \qquad (5)$$

where $\Delta x = x_i - x_{i-1}$. f_i and f'_i are updated approximately by eq. (2) with this polynomial and its spatial derivative as

$$f_i^* = F_i(x_i - c\Delta t) = a_i\xi^3 + b_i\xi^2 + f_i'\xi + f_i, \qquad (6)$$

$$f_i'^* = dF_i(x_i - c\Delta t)/dx = 3a_i\xi^2 + 2b_i\xi + f_i', \qquad (7)$$

where

$$\xi = -c\Delta t, \qquad (c \geq 0) \qquad (8)$$

and the superscript * means the time at $t+\Delta t$.

3. An implicit version of the CIP method

In extending this method to an implicit scheme, we need to forget temporarily a part of the concepts of the CIP method mentioned above, because the starting point eq. (2) that leads to eqs. (6) and (7) is merely a product of explicit thinking. In order to change our view point, we rewrite eqs. (6) and (7) as follows:

$$f_i^* = f_i + f_i'\xi + b_i\xi^2 + a_i\xi^3, \tag{9}$$

$$f_i'^* = f_i' + 2b_i\xi + 3a_i\xi^2. \tag{10}$$

Reminding that $\xi = -c\Delta t$, we can consider eq. (9) to be the Taylor expansion of f in time at n;

$$f^* = f + f_t\Delta t + f_{tt}\frac{\Delta t^2}{2} + f_{ttt}\frac{\Delta t^3}{6} + O(\Delta t^4). \tag{11}$$

In contrast, the Taylor expansion centered at * leads to

$$f^* = f + f_t^*\Delta t - f_{tt}^*\frac{\Delta t^2}{2} + f_{ttt}^*\frac{\Delta t^3}{6} + O(\Delta t^4). \tag{12}$$

From this analogy, we come to an implicit formulation of the CIP method;

$$f_i^* = f_i + f_i'^*\xi - b_i^*\xi^2 + a_i^*\xi^3, \tag{13}$$

and

$$f_i'^* = f_i' + 2b_i^*\xi - 3a_i^*\xi^2, \tag{14}$$

where

$$a_i^* = \frac{(f_i'^* + f_{i-1}'^*)}{\Delta x^2} - \frac{2(f_i^* - f_{i-1}^*)}{\Delta x^3}, \tag{15}$$

$$b_i^* = \frac{(2f_i'^* + f_{i-1}'^*)}{\Delta x} - \frac{3(f_i^* - f_{i-1}^*)}{\Delta x^2}. \tag{16}$$

We can prove that the Taylor expansion eq. (11) in time is equivalent to eq. (9). Substituting eq. (8) into eq. (9), we obtain the following equation:

$$f_i^* = f_i - f_i' c\Delta t + b_i c^2 \Delta t^2 - a_i c^3 \Delta t^3. \tag{17}$$

When the spatial profile is expanded into Taylor series and is compared with the cubic polynomial eq. (6), we get

$$2b_i = f_i'' + O(\Delta x^2), \qquad \text{and} \qquad 6a_i = f_i''' + O(\Delta x). \tag{18}$$

These spatial derivatives can be transformed to the temporal derivatives as

$$f_{tt} = c^2 f'', \qquad \text{and} \qquad f_{ttt} = -c^3 f''', \tag{19}$$

by taking derivatives of eq. (1). Thus we retrieve eq. (11). We can derive the same result from eq. (2) because this equation means that the spatial profile of f corresponds to the temporal profile of f. This justifies the use of analogy between eqs. (12) and (13).

The solution of eqs. (13) and (14) is rewritten as

$$f_i^* = \frac{\kappa(\kappa+1)(\kappa f_{i-1}'^{\,*} - f_i')\Delta x + \kappa^2(\kappa+3)f_{i-1}^{\,*} + (3\kappa+1)f_i}{(\kappa+1)^3}, \tag{20}$$

and

$$f_i'^{\,*} = \frac{(\kappa+1)\{\kappa(\kappa-2)f_{i-1}'^{\,*} - (2\kappa-1)f_i'\} - 6\kappa(f_{i-1}^{\,*} - f_i)/\Delta x}{(\kappa+1)^3}, \tag{21}$$

where κ is the CFL number:

$$\kappa = -\frac{\xi}{\Delta x}. \tag{22}$$

Equations (20) and (21) can be solved explicitly in the order of increasing i. In the above discussions, we treat only the case $c \geq 0$, so we must change eqs. (20)–(22) as $i-1 \Rightarrow i+1$ and $\Delta x \Rightarrow -\Delta x$ in the case $c < 0$, and these equations are solved in the order of decreasing i.

4. Numerical results

We first apply this method to the propagation of a square wave. All results shown below are at the time when the wave moves by a distance $200\Delta x$ from its initial position and the CFL number or the time step Δt is linearly increased from 0 to specified values during first several steps. Figure 1 shows the results for low CFL number with explicit and implicit CIPs. The results with the implicit CIP are quite similar to those with the previous explicit CIP. Figure 2 shows the results for various high CFL numbers. Even with an extremely high CFL number, this method provides stable results.

In these computations, we know that the accuracy of the implicit CIP is same as that of the previous CIP, and this method is stable with any CFL numbers.

We can also use the variable-transformation technique [9] with a tangent function coupled with the implicit CIP as done with the explicit CIP. This technique is very effective in the case when we use the solution of eq. (1) as the density function (or the color function) which describes the interface between different materials. Here we use a transformation:

$$\phi = (\arctan f)/(0.99\pi) + 0.5, \tag{23}$$

$$f = \tan[0.99\pi(\phi - 0.5)], \tag{24}$$

where ϕ works as the density function whose range is 0.0~1.0. Stable calculation but significant diffusion for high CFL number is a nature of any implicit schemes. We should note that most important point is stable nature when the implicit schemes are requested. Even in this case, however, the variable-transformation technique can greatly reduce the diffusion. Figure 3 shows the results with these procedures. Even in the case that CFL number is set to 2.0 which is 10 times larger than that frequently used for explicit CIP, the configuration of the square wave is kept well for a long time.

Next, we apply this method combined with the CUP procedure [10] to the one-dimensional shock-tube problem . The conditions are same as in ref. 3 except near the right-side boundary where we put a region expanding with quite a high velocity u = 13.0 and u is fixed on the boundary. This perturbation causes an expansion wave whose velocity is about ten times larger than that of the shock wave generated in the central region. If we are not interested in this expansion wave and we want to control the time step with the velocity of the shock wave, not of the expansion wave, we need an implicit scheme described above. Figure 4 (a) and (b) show the density profile at t = 0.0 and t = 0.275, respectively. In this case, we set CFL = 1.3 at the expansion region. For comparison, we show the result for a low CFL number (CFL = 0.2) in fig. 4 (c). These two results are quite similar, while the total CPU time for the computation of (b) is 6.5 times smaller than that of (c).

5. Conclusion

We have proposed an implicit version of the CIP method. This method provides a less diffusive result in a low-CFL computation and is stable even in a extremely-high-CFL computation.

Note that the main equations of this implicit scheme, eqs. (20) and (21), are the two-points connected systems although this scheme has 3rd-order accuracy. Because of this fact, if we treat the boundary conditions carefully, the CIP scheme, even with an implicit form, can be solved without any matrix solvers even in general cases, for example, when the direction of the velocity is not uniform in space. The extension to higher-dimensions is possible by a directional splitting technique. We will discuss this matter in a future paper.

Acknowledgement

This work was carried out under the collaborating research program at the National Institute for Fusion Science.

References

[1] H. Takewaki, A. Nishiguchi and T. Yabe, J. Comput. Phys. 61 (1985) 261.

[2] T. Yabe and E. Takei, J. Phys. Soc. Japan. 57 (1988) 2598.

[3] T. Yabe and T. Aoki, Comput. Phys. Commun. 66 (1991) 219.

[4] T. Yabe, T. Ishikawa, P. Y. Wang, T. Aoki, Y. Kadota and F. Ikeda, Comput. Phys. Commun. 66 (1991) 233.

[5] R. Beam and R. F. Warming, AIAA Paper. 77 (1977) 645.

[6] R. W. MacCormack, *AIAA. J.* 20 (1982) 9.

[7] U. C. Yee, J. Comput. Phys. 68 (1987) 151.

[8] P. Steinle and R. Morrow, J. Comput. Phys. 80 (1989) 61.

[9] T. Yabe and F. Xiao, J. Phys. Soc. Japan. 62 (1993) 2537.

[10] T. Yabe and P. Y. Wang, J. Phys. Soc. Japan. 60 (1991) 2105.

FIGURE CAPTIONS

Fig.1 Linear wave propagation with (a) an explicit and (b) implicit CIP with CFL = 0.2. The symbols and solid lines denote numerical and analytical solutions, respectively.

Fig.2 Linear wave propagation with implicit CIP with (a) CFL = 1.0, (b) CFL = 2.0, (c) CFL = 5.0 and (d) CFL = 20.0. The symbols and solid lines denote numerical and analytical solutions, respectively.

Fig.3 Linear wave propagation with implicit CIP combined with the variable transformation. CFL numbers are set to (a) 1.0, (b) 2.0 and (c) 4.0. The symbols and solid lines denote numerical and analytical solutions, respectively.

Fig.4 One-dimensional shock-tube problem. Figures show the density profile at t = 0.0 (a), t = 0.276 with CFL = 1.3 (b) and t = 0.276 with CFL = 0.2 (c). The symbols denote numerical results and solid lines denote an analytical solution without expansion region.

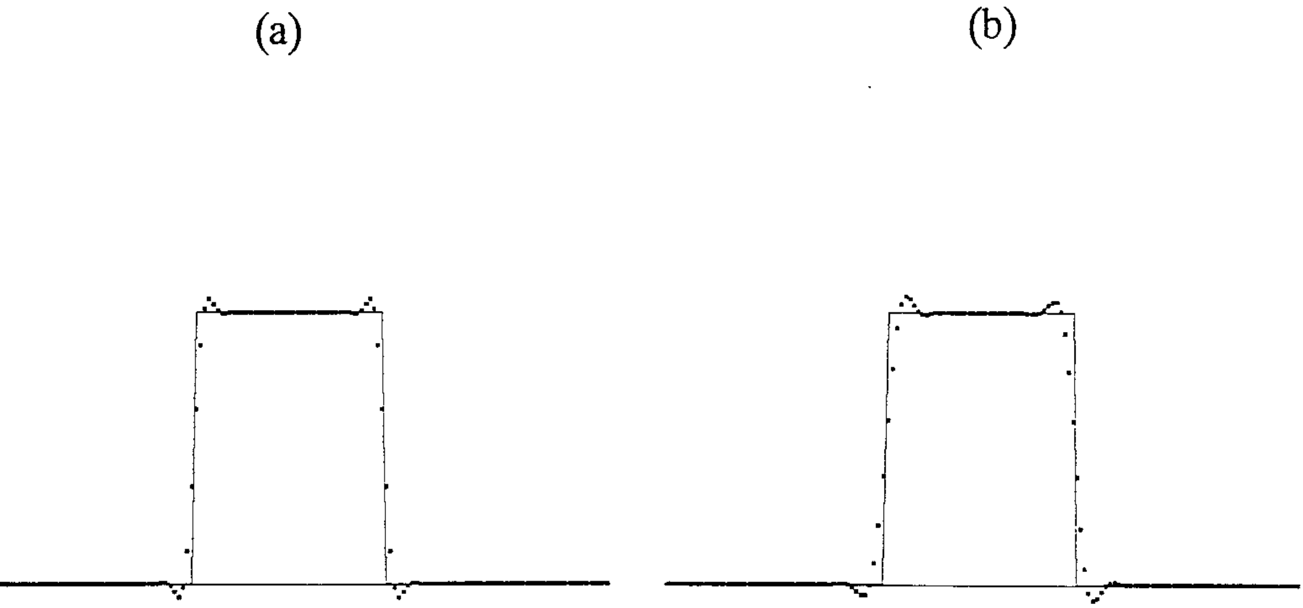

Fig.1

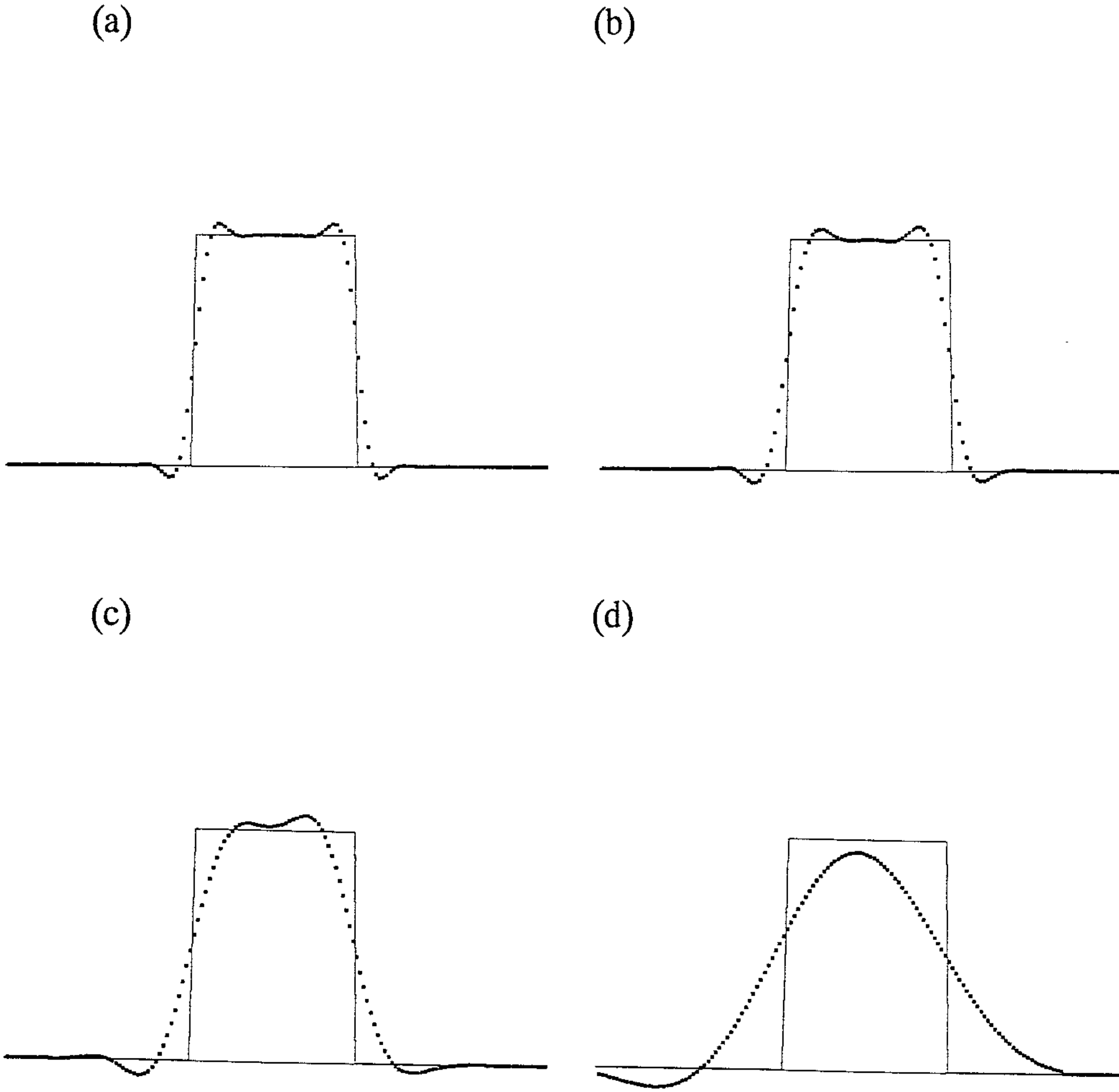

Fig.2

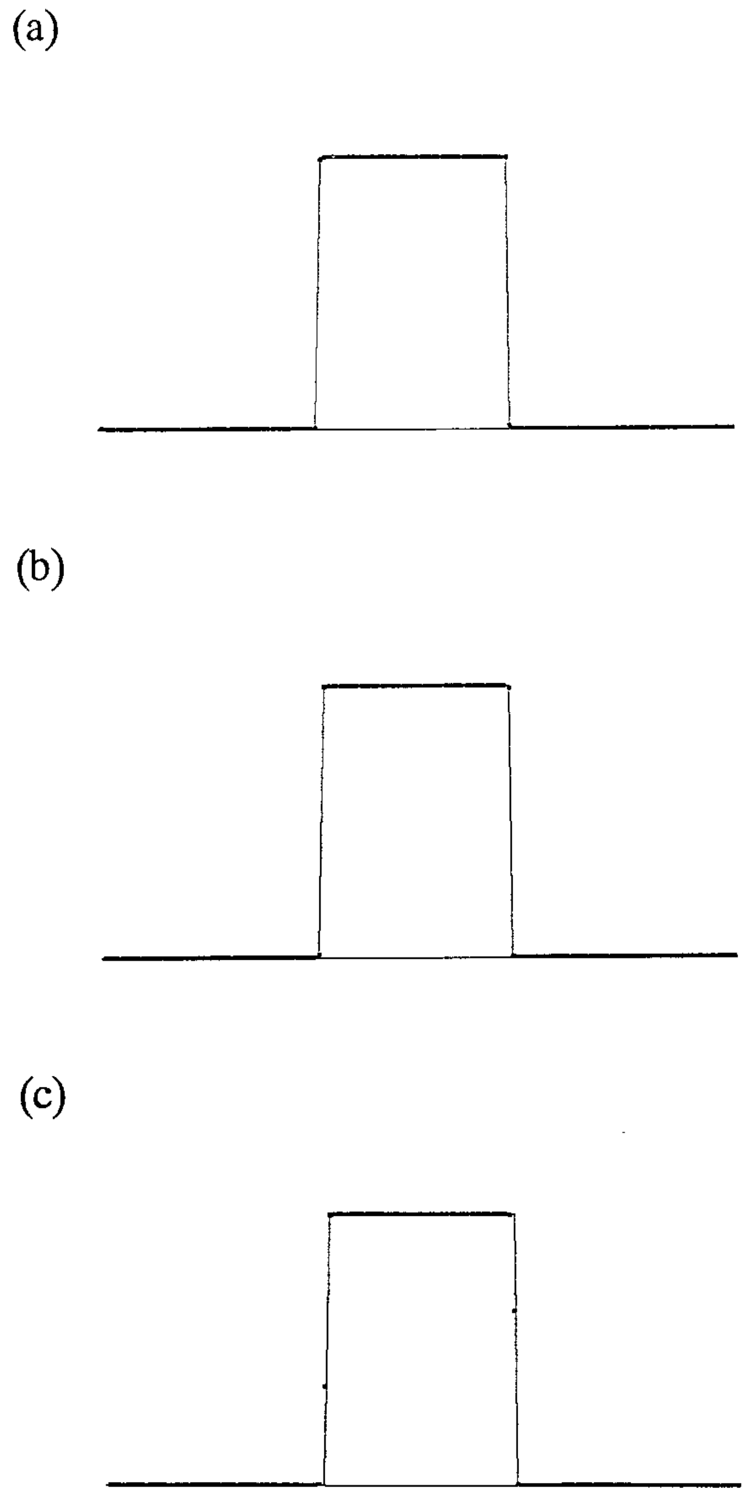

Fig.3

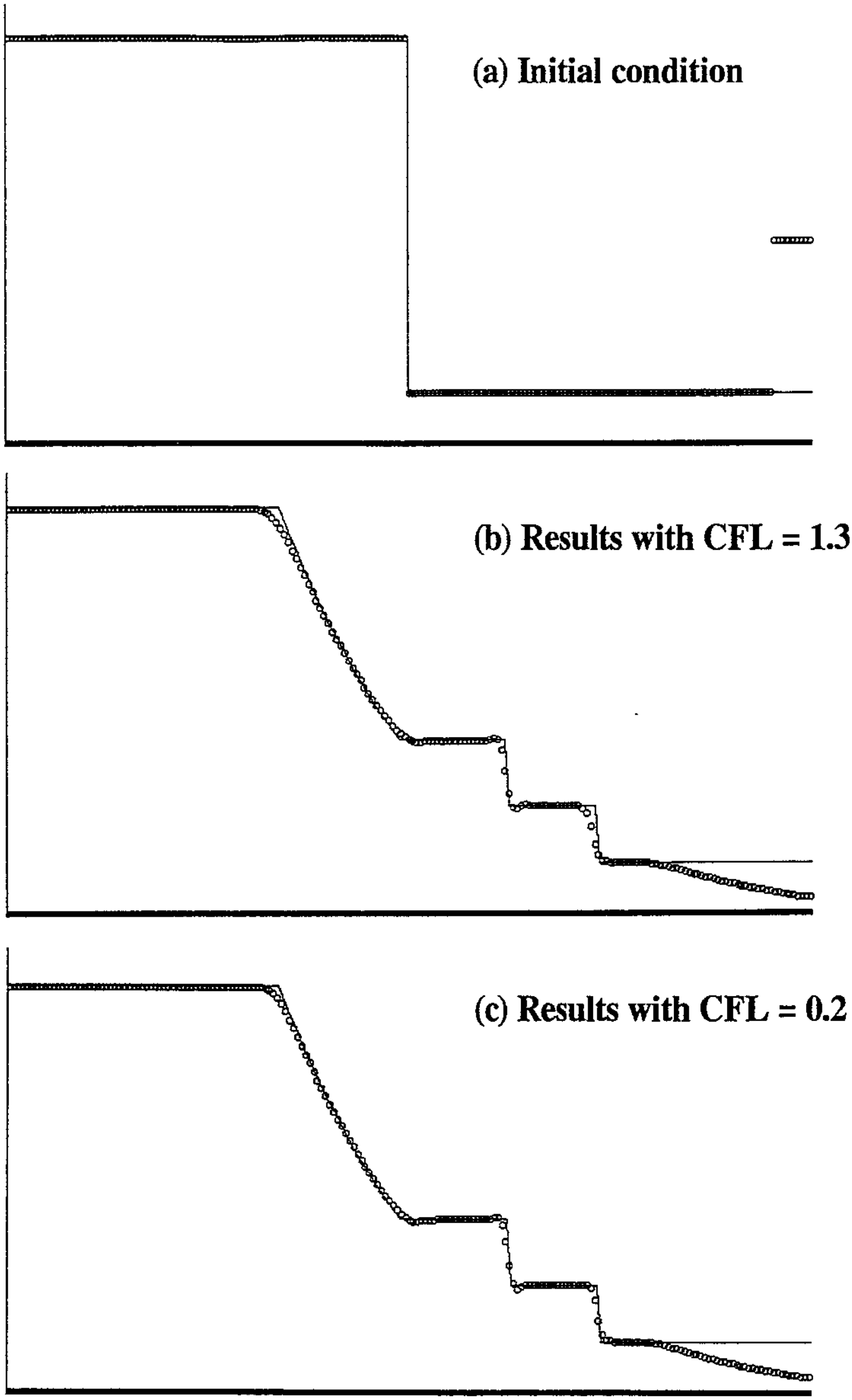
(a) Initial condition
(b) Results with CFL = 1.3
(c) Results with CFL = 0.2

Fig.4

Recent Issues of NIFS Series

NIFS-309 H. Amo, T. Sato and A. Kageyama,
Intermittent Energy Bursts and Recurrent Topological Change of a Twisting Magnetic Flux Tube; Sep.1994

NIFS-310 T. Yamagishi and H. Sanuki,
Effect of Anomalous Plasma Transport on Radial Electric Field in Torsatron/Heliotron; Sep. 1994

NIFS-311 K. Watanabe, T. Sato and Y. Nakayama,
Current-profile Flattening and Hot Core Shift due to the Nonlinear Development of Resistive Kink Mode; Oct. 1994

NIFS-312 M. Salimullah, B. Dasgupta, K. Watanabe and T. Sato,
Modification and Damping of Alfvén Waves in a Magnetized Dusty Plasma; Oct. 1994

NIFS-313 K. Ida, Y. Miura, S -I. Itoh, J.V. Hofmann, A. Fukuyama, S. Hidekuma, H. Sanuki, H. Idei, H. Yamada, H. Iguchi, K. Itoh,
Physical Mechanism Determining the Radial Electric Field and its Radial Structure in a Toroidal Plasma; Oct. 1994

NIFS-314 Shao-ping Zhu, R. Horiuchi, T. Sato and The Complexity Simulation Group,
Non-Taylor Magnetohydrodynamic Self-Organization; Oct. 1994

NIFS-315 M. Tanaka,
Collisionless Magnetic Reconnection Associated with Coalescence of Flux Bundles; Nov. 1994

NIFS-316 M. Tanaka,
Macro-EM Particle Simulation Method and A Study of Collisionless Magnetic Reconnection; Nov. 1994

NIFS-317 A. Fujisawa, H. Iguchi, M. Sasao and Y. Hamada,
Second Order Focusing Property of 210° Cylindrical Energy Analyzer; Nov. 1994

NIFS-318 T. Sato and Complexity Simulation Group,
Complexity in Plasma - A Grand View of Self- Organization; Nov. 1994

NIFS-319 Y. Todo, T. Sato, K. Watanabe, T.H. Watanabe and R. Horiuchi,
MHD-Vlasov Simulation of the Toroidal Alfvén Eigenmode; Nov. 1994

NIFS-320 A. Kageyama, T. Sato and The Complexity Simulation Group,
Computer Simulation of a Magnetohydrodynamic Dynamo II: Nov. 1994

NIFS-321 A. Bhattacharjee, T. Hayashi, C.C.Hegna, N. Nakajima and T. Sato,
Theory of Pressure-induced Islands and Self-healing in Three-

dimensional Toroidal Magnetohydrodynamic Equilibria; Nov. 1994

NIFS-322 A. Iiyoshi, K. Yamazaki and the LHD Group,
Recent Studies of the Large Helical Device; Nov. 1994

NIFS-323 A. Iiyoshi and K. Yamazaki,
The Next Large Helical Devices; Nov. 1994

NIFS-324 V.D. Pustovitov
Quasisymmetry Equations for Conventional Stellarators; Nov. 1994

NIFS-325 A. Taniike, M. Sasao, Y. Hamada, J. Fujita, M. Wada,
The Energy Broadening Resulting from Electron Stripping Process of a Low Energy Au^- *Beam;* Dec. 1994

NIFS-326 I. Viniar and S. Sudo,
New Pellet Production and Acceleration Technologies for High Speed Pellet Injection System "HIPEL" in Large Helical Device; Dec. 1994

NIFS-327 Y. Hamada, A. Nishizawa, Y. Kawasumi, K. Kawahata, K. Itoh, A. Ejiri, K. Toi, K. Narihara, K. Sato, T. Seki, H. Iguchi, A. Fujisawa, K. Adachi, S. Hidekuma, S. Hirokura, K. Ida, M. Kojima, J. Koong, R. Kumazawa, H. Kuramoto, R. Liang, T. Minami, H. Sakakita, M. Sasao, K.N. Sato, T. Tsuzuki, J. Xu, I. Yamada, T. Watari,
Fast Potential Change in Sawteeth in JIPP T-IIU Tokamak Plasmas; Dec. 1994

NIFS-328 V.D. Pustovitov,
Effect of Satellite Helical Harmonics on the Stellarator Configuration; Dec. 1994

NIFS-329 K. Itoh, S-I. Itoh and A. Fukuyama,
A Model of Sawtooth Based on the Transport Catastrophe; Dec. 1994

NIFS-330 K. Nagasaki, A. Ejiri,
Launching Conditions for Electron Cyclotron Heating in a Sheared Magnetic Field; Jan. 1995

NIFS-331 T.H. Watanabe, Y. Todo, R. Horiuchi, K. Watanabe, T. Sato,
An Advanced Electrostatic Particle Simulation Algorithm for Implicit Time Integration; Jan. 1995

NIFS-332 N. Bekki and T. Karakisawa,
Bifurcations from Periodic Solution in a Simplified Model of Two-dimensional Magnetoconvection; Jan. 1995

NIFS-333 K. Itoh, S.-I. Itoh, M. Yagi, A. Fukuyama,
Theory of Anomalous Transport in Reverse Field Pinch; Jan. 1995

NIFS-334 K. Nagasaki, A. Isayama and A. Ejiri
Application of Grating Polarizer to 106.4GHz ECH System on Heliotron-E; Jan. 1995

NIFS-335 H. Takamaru, T. Sato, R. Horiuchi, K. Watanabe and Complexity Simulation Group,
A Self-Consistent Open Boundary Model for Particle Simulation in Plasmas; Feb. 1995

NIFS-336 B.B. Kadomtsev,
Quantum Telegragh : is it possible?; Feb. 1995

NIFS-337 B.B.Kadomtsev,
Ball Lightning as Self-Organization Phenomenon; Feb. 1995

NIFS-338 Y. Takeiri, A. Ando, O. Kaneko, Y. Oka, K. Tsumori, R. Akiyama, E. Asano, T. Kawamoto, M. Tanaka and T. Kuroda,
High-Energy Acceleration of an Intense Negative Ion Beam; Feb. 1995

NIFS-339 K. Toi, T. Morisaki, S. Sakakibara, S. Ohdachi, T.Minami, S. Morita, H. Yamada, K. Tanaka, K. Ida, S. Okamura, A. Ejiri, H. Iguchi, K. Nishimura, K. Matsuoka, A. Ando, J. Xu, I. Yamada, K. Narihara, R. Akiyama, H. Idei, S. Kubo, T. Ozaki, C. Takahashi, K. Tsumori,
H-Mode Study in CHS; Feb. 1995

NIFS-340 T. Okada and H. Tazawa,
Filamentation Instability in a Light Ion Beam-plasma System with External Magnetic Field; Feb. 1995

NIFS-341 T. Watanbe, G. Gnudi,
A New Algorithm for Differential-Algebraic Equations Based on HIDM; Feb. 13, 1995

NIFS-342 Y. Nejoh,
New Stationary Solutions of the Nonlinear Drift Wave Equation; Feb. 1995

NIFS-343 A. Ejiri, S. Sakakibara and K. Kawahata,
Signal Based Mixing Analysis for the Magnetohydrodynamic Mode Reconstruction from Homodyne Microwave Reflectometry; Mar.. 1995

NIFS-344 B.B.Kadomtsev, K. Itoh, S.-I. Itoh
Fast Change in Core Transport after L-H Transition; Mar. 1995

NIFS-345 W.X. Wang, M. Okamoto, N. Nakajima and S. Murakami,
An Accurate Nonlinear Monte Carlo Collision Operator; Mar. 1995

NIFS-346 S. Sasaki, S. Takamura, S. Masuzaki, S. Watanabe, T. Kato, K. Kadota,
Helium I Line Intensity Ratios in a Plasma for the Diagnostics of Fusion

Edge Plasmas; Mar. 1995

NIFS-347 M. Osakabe,
Measurement of Neutron Energy on D-T Fusion Plasma Experiments; Apr. 1995

NIFS-348 M. Sita Janaki, M.R. Gupta and Brahmananda Dasgupta,
Adiabatic Electron Acceleration in a Cnoidal Wave; Apr. 1995

NIFS-349 J. Xu, K. Ida and J. Fujita,
A Note for Pitch Angle Measurement of Magnetic Field in a Toroidal Plasma Using Motional Stark Effect; Apr. 1995

NIFS-350 J. Uramoto,
Characteristics for Metal Plate Penetration of a Low Energy Negative Muonlike or Pionlike Particle Beam: Apr. 1995

NIFS-351 J. Uramoto,
An Estimation of Life Time for A Low Energy Negative Pionlike Particle Beam: Apr. 1995

NIFS-352 A. Taniike,
Energy Loss Mechanism of a Gold Ion Beam on a Tandem Acceleration System: May 1995

NIFS-353 A. Nishizawa, Y. Hamada, Y. Kawasumi and H. Iguchi,
Increase of Lifetime of Thallium Zeolite Ion Source for Single-Ended Accelerator: May 1995

NIFS-354 S. Murakami, N. Nakajima, S. Okamura and M. Okamoto,
Orbital Aspects of Reachable β *Value in NBI Heated Heliotron/Torsatrons;* May 1995

NIFS-355 H. Sugama and W. Horton,
Neoclassical and Anomalous Transport in Axisymmetric Toroidal Plasmas with Electrostatic Turbulence; May 1995

NIFS-356 N. Ohyabu
A New Boundary Control Scheme for Simultaneous Achievement of H-mode and Radiative Cooling (SHC Boundary); May 1995

NIFS-357 Y. Hamada, K.N. Sato, H. Sakakita, A. Nishizawa, Y. Kawasumi, R. Liang, K. Kawahata, A. Ejiri, K. Toi, K. Narihara, K. Sato, T. Seki, H. Iguchi, A. Fujisawa, K. Adachi, S. Hidekuma, S. Hirokura, K. Ida, M. Kojima, J. Koong, R. Kumazawa, H. Kuramoto, T. Minami,. M. Sasao, T. Tsuzuki, J.Xu, I. Yamada, and T. Watari,
Large Potential Change Induced by Pellet Injection in JIPP T-IIU Tokamak Plasmas; May 1995